Crosstalk Between Substance P and Calcitonin Gene-Related Peptide During Heterotopic Ossification in Murine Achilles Tendon

Ceren Tuzmen[1], **Kostas Verdelis**[2], **Lee Weiss**[3,4,5], and **Phil Campbell**[1,4,5,6]

[1]Department of Biological Sciences, Carnegie Mellon University, Pittsburgh, Pennsylvania

[2]Center for Craniofacial Regeneration, University of Pittsburgh, Pittsburgh, Pennsylvania

[3]Robotics Institute, Carnegie Mellon University, Pittsburgh, Pennsylvania

[4]Department of Biomedical Engineering, Carnegie Mellon University, Pittsburgh, Pennsylvania

[5]McGowan Institute for Regenerative Medicine, University of Pittsburgh, Pittsburgh, Pennsylvania

[6]Engineering Research Accelerator, Carnegie Mellon University, Pittsburgh, Pennsylvania

Abstract

Heterotopic ossification (HO) is abnormal bone formation within soft tissue, usually predisposed by neurogenic or musculoskeletal trauma. Inflammation resulting from trauma is considered to be the main trigger for HO by eliciting changes within the injury site, including elevation of bone morphogenetic proteins (BMPs). Recent research, however, has also associated changes in sensory neuropeptide expression with HO. Substance P (SP) and calcitonin gene-related peptide (CGRP) are two of those neuropeptides that have been implicated with various aspects of HO, including regulation of inflammation and BMP signaling. Despite discoveries associating SP and CGRP with soft tissue HO, it remains unclear whether SP and CGRP have a direct role in the induction of HO. Here, we investigated the effect of SP and CGRP in vivo with the aid of inkjet-based biopatterning technology to controllably deliver these neuropeptides onto a murine Achilles tendon. While we did not observe any significant effect with CGRP, SP alone promoted HO in vivo with increased expression of BMP2. Remarkably, when SP and CGRP were delivered together, CGRP counteracted the effect of SP and essentially blocked SP-induced HO. This report contributes to the understanding of the complex problem of HO pathophysiology and warrants more study to better elucidate the interplay between SP and CGRP in the induction of HO.

Keywords

heterotopic ossification; substance P; calcitonin gene-related peptide; bone morphogenetic protein 2; inflammation

Heterotopic ossification (HO) is bone formation at an anatomic site where bone normally does not exist. It is increasingly recognized as a clinically significant problem, where up to 20% of patients develop severe limitations in mobility, affecting their quality of life.[1] Surgery is the only treatment option for patients with matured HO, however, it has been associated with other complications, such as increased risk of infection or unsuccessful wound healing, and recurrence rates of HO are high.[1] Use of non-steroidal antiinflammatory drugs (NSAIDs) and radiotherapy has been shown to reduce HO after neurogenic or orthopedic trauma, but neither of these options are fully effective nor can they prevent it. The biggest challenge in development of therapies for HO has been inadequate understanding of the pathophysiology of HO. Current animal models of HO lack precise control over specific signaling molecules thus confounding interpretation of outcomes and motivating the need for more highly controlled experimental models.[2,3]

The most common causes of HO are traumatic injuries, either to the musculoskeletal tissues or to the central nervous system.[4–6] The etiology involves neovascularization and sometimes nerve innervation within a soft tissue, followed by recruitment of inflammatory immune cells and possibly osteoprogenitor stem cells from neighboring tissues.[1,4,5,7] According to recent data, particularly from the military, acute inflammation appears to be a critical component of trauma-driven HO.[4,5,7–9] Another similarity across all of the different types of HO, including its genetic disorders, is increased expression of bone morphogenetic proteins (BMPs).[4,10] Release of BMPs following inflammation is part of the standard healing mechanisms in musculoskeletal tissues.[10,11] However, elevated levels of BMP expression promote bone formation within soft tissues.

Previous research has also associated HO with changes in expression of other homeostatic factors including the sensory neuropeptides substance P (SP) and calcitonin gene-related peptide (CGRP).[12–17] SP and CGRP have immunoregulatory actions that are directly linked to HO pathophysiology, such as immune cell recruitment, cytokine release, vascularization, or nerve remodeling.[14,18–30] Correspondingly, SP and CGRP up-regulation has been observed with tendon trauma in clinical studies and in animal disease models, during the inflammatory phase.[16,18–21,23,25,31–33] Additionally, recent work also suggested neurogenic inflammation through activation of mast cells and macrophages play critical roles in HO induction. Depletion of injury-related macrophages and mast cells, through both chemical and genetic techniques, markedly suppressed ectopic bone formation in muscle HO models.[14,17,34] SP and CGRP have also been shown to interact with the BMPs, particularly BMP2 and BMP4, two of the main BMPs involved in HO.[14,15,24,35] In vitro studies have shown a correlation between SP, CGRP, and the BMP signaling, where both neuropeptides up-regulated BMP2 expression and osteogenic differentiation in osteoprogenitor stem cells.[27,36,37] Therefore, further elucidating the relationship between SP, CGRP, and HO could potentially lead to development of effective HO therapies.

In this study, we delivered SP and CGRP to uninjured murine Achilles tendons in order to investigate if they have a direct role in the induction of HO. To accomplish this, we used inkjet-based biopatterning technology for highly controlled and localized delivery of SP and CGRP, both individually and in combination. In contrast to conventional delivery methods,

such as systemic or localized injections or genetic manipulation, which lack precision and persistence of delivered signaling molecules, biopatterning enables controlled, spatial delivery of signaling molecules through their native binding to extracellular matrix (ECM) delivery vehicles. We have previously shown that acellular DermaMatrix (ADM) delivery vehicles biopatterned with other types of signaling molecules can be used to drive cells toward targeted fates in spatial registration to printed patterns, both in vitro and in vivo, at a millimeter scale resolution and at nanogram-level doses.[38–42] Having such control facilitates more precise interpretation and understanding of the biological significance of experimental outcomes. Here, biopatterning enabled a novel experimental model of HO induction that mimics localized up-regulation of neuropeptides in response to trauma. Until now the interplay between SP and CGRP in relation to HO has been based on associative studies. Being the first study that uses spatial administration of SP and CGRP to an uninjured tendon to determine their direct effect on HO, our work adds to the understanding of the pathophysiology of HO.

METHODS

Treatment Preparation and Use

SP (Bachem, Torrance, CA) and CGRP (Bachem) were reconstituted according to manufacturer's instructions to 1 mg/ml, aliquoted and stored at −80°C. Prior to use, they were freshly diluted to the desired concentration in 10mM sodium phosphate, pH 7.4.

Biopatterning

Treatments (biological inks or "bio-inks") were deposited onto 0.2mm thick DermaMatrix™ ADM sheets (Musculoskeletal Transplant Foundation, Edison, NJ) using our custom inkjet-based bioprinter.[38–43] Individual treatments consisting of SP or CGRP bioinks prepared in 10mM sodium phosphate were printed onto dry ADM sheets. Mid-sections of ADM sheets (2×4mm on 2×8mm strips) were biopatterned with SP, CGRP, or both, as shown in Figure 1A, using the previously reported protocol.[39] The protocol uses an "overprinting" strategy to modulate the deposited concentrations of signaling molecules, whereby each location on a pattern is overprinted with multiple droplets of dilute bioinks. The droplets absorb into the porous scaffold, and as the aqueous-based solvent evaporates, the signaling molecules contained in the bioinks become immobilized in the ADM due to their native binding affinities. This increases deposited concentrations in direct proportion to the number of overprints.[38] For this study, deposited drop sizes were measured using a drop-inflight JetXpert™ analysis system (Imagexpert, Inc., Nashua, NH). Based on those measurements, the total deposited dose for each neuropeptide was calculated to be 0.40μg/construct or ~47 ng/mm^2 (Table 1).

Binding and Retention of SP and CGRP

Radiolabeling was used to quantify binding and binding retention of neuropeptides to ADM as previously described but with modification.[42] Briefly, SP and CGRP were iodinated using chloramine T method, and ^{125}I-SP and ^{125}I-CGRP were separated from unincorporated ^{125}I using Bio-Gel P-4 size exclusion polyacrylamide gel beads (Bio-Rad, Hercules, CA). ADM samples, ~1mm×2mm, were incubated with either ^{125}I-SP or ^{125}I-CGRP in 20 μl of 100mM

sodium phosphate, pH 7.4 for 1 h, 37°C. ADM samples were rinsed three times with PBS, 21°C, aspirating PBS supernatant between rinses. ^{125}I-SP or ^{125}I-GCRP bound was determined by counting in Cobra auto-gamma counter (Perkin-Elmer, Wellesley, MA). The resulting radioactive counts represented initial bound neuropeptide. Simulated body fluid (SBF), MEM supplemented with 10% fetal bovine serum, 25mM HEPES, 0.02% sodium azide, 100 U/ml penicillin, and 100μg/ml streptomycin, were then added to ADM samples. At various times, SBF was aspirated, replaced with fresh SBF and bound radioactivity determined. Binding retention of radiolabeled neuropeptides is presented in Figure 1C. The curves represent the mean ± SEM of four individual experiments for each neuropeptide. Data were corrected for radioactive decay. Binding experiments were conducted independently at different timepoints for ^{125}I-SP and ^{125}I-CGRP.

Animals

C57BL/6 males, 3–4 months old, about 30–35g, were purchased from the Charles River (Wilmington, MA) and housed at the Mellon Institute Animal Facility in accordance with the regulations of the American Association for the Accreditation of Laboratory Animal Care according to the protocol AS15-039.

Surgeries

The animals were anaesthetized with the use of 2–3% isoflurane. Achilles tendons (left limb) of mice were surgically exposed ($n = 6$/group) and a tunnel was drilled through the calcaneus as an anchor point for suturing. Constructs were soaked in PBS 20–30min before implantation. The unprinted regions of ADM were sutured to the calcaneus and to the gastrocnemius, while the biopatterned region was placed over of the Achilles tendon (Fig. 1B). The tendon was not injured. Following the surgery, the animals were given Ibuprofen for pain through their drinking water. Locomotion, grooming, and eating habits of the surgically treated animals were monitored. Any animals found to be in distress during the study period were euthanized and excluded from the study. Animals were housed in cages (three animals/cage) and euthanized at 6 weeks via CO_2 asphyxiation and the treated legs were collected and fixed in 4% formalin.

Micro Computed Tomography (microCT)

Lower legs were rinsed to replace formalin with 70% ethanol then imaged using an in vivo VivaCT 40 (Scanco Medical, Brutisselen, Switzerland) microCT system, placed inside the manufacturer-provided tube holder in ethanol and stabilized with Parafilm. The scans were done with a 30 μm voxel resolution, a 55KVp beam energy, 145 μA current intensity, and 100ms exposure. Three-dimensional reconstruction of the lateral projections were performed using the Scanco software from the raw files and the resulting volumes were processed with the Scanco microCT 3D morphometry and densitometry software, operated in an open VMS environment. Regions of interest (ROIs) were defined around the heterotopic bone mass from the calcaneus bone to the suture site on gastrocnemius on sequential 2D views, with the resulting volume designated as tissue volume (TV), while the calculated total volume of heterotopic bone nodules after segmentation from the surrounding soft tissue and background was designated as bone volume (BV). An average mineral density value of

180mg/cc, representing a value lower than the mineralized tissue peak by 40% of the distance between the mineralized tissue and the soft tissue peaks, was used for segmentation.

Histological Analysis

Tissue samples were processed on an automated tissue processor by the University of Pittsburgh Histology Core Facility (Pittsburgh, PA). Briefly, the samples were first removed from the fixative (4% formalin) and placed through a series of graded alcohols, cleared through xylene and subsequently infiltrated with paraffin on the processor with vacuum. Upon removal from the automated processor, tissues were hand-embedded in paraffin. Once the paraffin blocks solidified, they were placed on ice and cut using a microtome to generate 5μm sections. These tissue sections were floated on a water bath and then collected onto positively charged slides which were baked in a 60°C oven for 1 h. Slides were stained for hematoxylin and eosin (H&E) according to the manufacturer's instructions. 1% Toluidine Blue stock solution was mixed with 1% Sodium Chloride to prepare Toluidine Blue working solution (pH 2.3–2.5). Deparaffinized and hydrated sections were stained for 3–4min at room temperature followed by dehydration through gradual ethanol and Xylene washes. 2% Fast Green solution was used as a counterstain. 1% Alcian Blue Solution was prepared in 3% glacial acetic acid along with 0.1% Nuclear Fast Red Solution. Sections were stained for Alcian Blue for 30min and for Nuclear Fast Red (counterstain) for 3 min at room temperature. Slides were dehydrated through serial ethanol and Xylene washes. 20× DIC images were taken on a Zeiss Axiovert 200M microscope (Carl Zeiss Microimaging, Thornwood, NY).

Immunolabeling

Mounted tissue sections on glass slides were deparaffinized and hydrated by placing them through graded xylene and ethanol washes. For antigen retrieval, they were boiled in Sodium Citrate Buffer (10mm Sodium Citrate, 0.05% Tween 20 (all from Sigma–Aldrich, St. Louis, MO), pH 6.0) for 10–15 min. Immunohistochemistry was performed using the EXPOSE rabbit-specific HRP/diaminobenzidine detection immunohistochemistry kit (Abcam, Cambridge, MA). Sections were incubated with antibody against BMP2 (Abcam) at a 1:200 dilution (overnight at 4°C). Hematoxylin was used as a counterstain. After dehydration through another series of xylene and ethanol washes, the sections were mounted in and imaged using a Zeiss Axiovert 200M microscope (Carl Zeiss Microimaging). For the immunofluorescence experiments, after deparaffinization and dehydration, the slides were blocked with 10% donkey serum (Jackson Immunoresearch, West Gove, PA) for 30 min at room temperature followed by additional blocking with 100 μg/ml donkey anti-mouse FAB (Jackson Immunoresearch) for 1 h at room temperature. Rat antimouse CD86 (B7-2) (1:100) and rabbit anti-mouse CD163 (1:100; both Santa Cruz Biotechnology Inc., Santa Cruz, CA) used as primary antibodies and Alexa Fluor® 488-donkey anti-rat and Cy5-donkey anti-rabbit (both 1:200; Jackson Immunoresearch, West Gove, PA) used as secondary antibodies. The stained sections were then mounted in Prolong Gold mounting medium (Invitrogen, CA) and imaged on Zeiss LSM 880 confocal laser scanning microscope (Carl Zeiss Microimaging).

Statistical Analysis

For statistical analysis, all data was subjected to Analysis of Variance (ANOVA) followed by Tukey's Post Hoc test for multiple comparison between each treatment group and the controls using MATLAB. Statistical significance was defined at p 0.05.

RESULTS

Delivery of SP and CGRP Using Biopatterning

To determine whether SP and/or CGRP promote HO in murine Achilles tendon, mid-sections of ADM strips were biopatterned with SP, CGRP or both (Fig. 1A). Total deposited dose of each neuropeptide was 0.40μg/construct (~47 ng/mm^2) as listed on Table 1. Biopatterned ADM constructs were implanted onto the left Achilles of 3–4 months-old male mice (Fig. 1B).

Binding retention conducted under simulated in vivo conditions demonstrated retention for SP at $46 \pm 0.57\%$ and CGRP at $52 \pm 0.67\%$ of initial neuropeptide bound to ADM after 24 hours. This reflects an approximate release of 50% of the neuropeptides on day 1, followed by an additional ~10 % release on day 2. Starting on day 3, there was an average release of both neuropeptides of ~1%/day until day 21, with $22 \pm 0.13\%$ of SP and $26.3 \pm 0.28\%$ of CGRP remaining bound to ADM (Fig. 1C). Extrapolating to in vivo, we delivered ~22 ng/mm^2 of SP and ~24 ng/mm^2 of CGRP within the first 24 h and an additional ~5 ng/mm^2 of each within the next 24 h.

SP Promoted HO While CGRP Blocked SP-Induced HO When Delivered Together

Control groups that received unpatterned (no treatment) ADM did not exhibit HO near the tendon 6 weeks postsurgery, according to the microCT results (Fig. 2A). Quantification of bone volume around the surgical sites, including the calcaneus and the Achilles, showed significant bone formation (p 0.001) in SP delivered legs compared to controls as well as all other experimental groups. CGRP did not have any significant effect ($p = 0.9$) compared to the controls (Fig. 2A and B). Animals that received combination of SP and CGRP showed significant reduction in HO compared to animals that received SP (p 0.001) (Fig. 2A and B). HO expressed as bone density (BV/TV) as shown to be higher in tendons upon SP delivery, while this was not observed in other treatment groups (p 0.01) (Fig. 2C).

Histological Analysis Revealed Endochondral Bone and Inflammatory Changes in Tendons That Received SP

Histology of the decalcified legs after 6 weeks revealed multiple sites of de novo bone tissue in tendons that received SP treatment. These sites exhibited nodules of lamellar bone tissue surrounded by high number of chondrocytes; therefore, HO occurred through endochondral ossification (Fig. 3B, F, and I). Alcian Blue and Toluidine Blue stains were used to confirm chondrocyte differentiation around the heterotopic bones (Fig. 4B and F). H&E staining of the tendon sections revealed marked differences between the tendons that received SP and other experimental groups (Fig. 3A–D). Delivery of SP resulted in degeneration of the tendon tissue, with vascularization and cellular infiltration within these tendons (Fig. 3B, F,

and I). These observations imply induction of inflammatory response, consistent with the related work suggesting that inflammation is involved in HO pathophysiology.

Histological Analysis Showed Chondrocyte Differentiation but no HO in Tendons That Received CGRP and SP + CGRP

Similar inflammatory changes did not appear in tendons that received CGRP or the combination of SP and CGRP. This suggests possible modulation of SP-driven inflammation by CGRP (Fig. 3C–D, G–H, and J–K). Interestingly, although the microCT data showed mostly no heterotopic bone in these treatment groups, histology revealed chondrocyte differentiation. This was was also confirmed by Alcian Blue and Toluidine Blue stainings (Fig. 3C–D, G–H, J–K, and Fig. 4C–D and G–H). This implies initiation of endochondral ossification but further mitigation of bone differentiation, and therefore a potential crosstalk between SP and CGRP in the induction of HO.

BMP2 Expression was Up-Regulated Upon SP and/or CGRP Delivery

Up-regulation of BMP expression is another component of HO. Among the other BMPs, BMP2 has been shown not only to be involved in soft tissue HO but also to interact with SP and CGRP signaling.[14,15,36,37,44] To test whether the SP or CGRP induces HO through BMP up-regulation, or conversely the combination of SP and CGRP down-regulates BMP levels, we investigated BMP2 expression on treated tendons. All HO sites in SP-delivered tendons exhibited localized, enhanced BMP2 expression compared to the controls (Fig. 4J and K). Additionally, the chondrocytes appeared BMP2 positive in SP-, CGRP-, and SP + CGRP-delivered tendons (Fig. 4J, L, and N). Therefore, BMP2 was likely to be involved in the induction of endochondral ossification and HO through SP and/or CGRP delivery, both of which could upregulate endogenous BMP2.

Histological Changes Were Observed in Tendons That Received SP

Both SP and CGRP delivery induced pathological changes in the Achilles including increased mononuclear cell infiltration through the ADM compared to controls and the combination treatments. Mast cell granules were observed in the skin and connective tissue neighboring the tendon as well as in the ADM but not within the tendon (Fig. 5). Salisbury et al.[14] reported Mast cell accumulation after HO induction in a muscle model. Since tendon exhibits low blood supply, the Mast cells are likely to be recruited to the connective tissues around the tendon. However, no marked differences were observed across different treatment groups and the controls (Fig. 5). Since, the analyses were done at a later time-point, i.e. 6 week post-surgery, this might not be a surprising result, considering, inflammatory response typically clears in 2 weeks.

It was previously shown that ablation of inflammatory macrophages reduces HO formation in different animal models of HO.[17,34] Therefore, we also investigated the presence of M1 (pro-inflammatory) and M2 (pro-repair) macrophage sub-populations in the treated tendons. We observed a few M1 macrophages infiltrating through the ADM in all treatment groups. This result, together with the Mast cell staining, implies a foreign body response to ADM in all treatment groups (Fig. 6A–D). Conversely, M2 staining was very low in all treatment groups. No macrophage infiltration was observed other than the tendon borders, which were

mainly dominated by the M1 macrophages (Fig. 6). Both M1 and M2 staining, M1 being much higher in intensity, were positive in cells that reside in marrowlike cavities in HO sites (Fig. 6B and J). These monocytes have been shown to be positive for the markers we used for labeling M1 and M2 populations.[45,46] We also observed positive M1 macrophage staining around the HO sites in SP delivered tendons, although it is not certain whether these are vesicles growing into the tendon or new bone module formation (Fig. 6B and J).

DISCUSSION

The intent of this study was to determine whether highly controlled, localized delivery of exogenous SP and CGRP could induce HO in the Achilles. Unlike other models, this model did not involve exogenous BMP delivery or trauma to the tissue to induce HO. Biopatterning[39,41,42] of an ADM delivery vehicle with SP and CGRP facilitated spatial control of signal molecule delivery via their native binding affinities. This mitigated rapid clearance of these molecules if they had otherwise been delivered in the "liquid-phase" (i.e., soluble) using conventional methods such as systemic or local injections. Using biopatterning to create a novel experimental model of HO induction mimicked, in-part, the response to trauma-Driven up-regulation of these neuropeptides, which strengthens our conclusions regarding the biological role of SP and CGRP in soft tissue HO pathophysiology.[4,14,15]

We demonstrated a clear effect of SP delivery to induce HO by promoting degenerative changes and BMP2 up-regulation in murine Achilles tendon. The model without neuropeptide delivery did not induce HO. According to previous studies in our lab, we also did not observe HO in animals with only a tunnel in the calcaneus and without the ADM implanted (manuscript in preparation). While CGRP did not result in inflammation and significant HO, it could still up-regulate BMP2 expression and promote chondrocyte differentiation in the Achilles tendon. Co-delivery of SP and CGRP did not exhibit HO formation, although histological analysis still showed chondrocyte differentiation in these tendons. Therefore, endochondral ossification was initiated, but HO induction was suppressed, suggesting a possible crosstalk between SP and CGRP. The two neuropeptides, when deliered together, instead of resulting in additive effects, counteracted each other.

Inflammation is an important component of HO.[47] Use of NSAIDs following orthopedic trauma is able to reduce HO in 60% of the cases, which serves a clinical base for the contribution of inflammation to HO formation.[48] In addition, inflammation possibly plays a role in the induction of BMP up-regulation as part of the repair mechanisms. In a rat Achilles injury model, Ackerman et al.[31] showed up-regulation of SP and CGRP during the first 2 weeks, followed by down-regulation of both neuropeptides as inflammation resolves and the tendon starts to heal, with CGRP concentration being higher than SP.

Histological analysis of tendons that received the SP constructs exhibited degenerative changes in these tendons, such as vascularization and cellular proliferation/infiltration, suggesting inflammation. These changes were not observed in other treatment groups. Earlier studies have shown that SP can promote inflammatory changes in tendon, such as alteration in the collagen composition, cellular infiltration, or vascular growth, which is

consistent with this finding.[25,26,32] A recent report by Zhou et al.[27] showed upregulation of chondrogenic and osteogenic markers in tenocytes after stimulation with SP. SP injection into rat patella only showed disorganized tendon matrix; however, the analysis was done 2 weeks after the injections.[27] The same group also showed opposing dose-dependent effects of SP on tenocytes, where low doses of SP (0.5 nmol) induced proliferation and markedly increased expression of tenocyte markers. Higher doses (5 nmol) of SP, on the other hand, decreased expression of tenocyte markers and up-regulated expression of adipocyte, chondrocyte, or osteoblast markers.[49] Interestingly, SP injections into the paratenon of ruptured rat Achilles, along with neutral endopeptidase inhibitors, improved resistance to stress, as well as healing response with increased proliferation and collagen remodeling.[50,51] Carlsson et al.[26] showed that SP injections enhance tissue proliferation and regulate sensory nerve ingrowth on injured rat Achilles.[26] Similarly, Bring et al.[52] reported that higher residual SP levels can improve tensile strength and stress at failure through the course of healing following depletion of most of the SP/CGRP positive sensory neurons using capsaicin in rat Achilles combined with tenatomy. CGRP did not improve tissue repair in the same study.[52] These studies are in accordance with SP's wound healing capacity, yet contradicts numerous other studies showing that SP is associated with pathological changes in the tendon. Therefore, it is possible that while lower doses of SP enhance healing, higher doses have destructive effects on the tissue. Although the data indicate that SP alone can induce HO in uninjured Achilles tendon, there remains the possibility of SP having different effects in a traumatized tendon. As we did not incorporate tissue trauma in our model, the response induced by SP might be different in healing versus healthy tissues.

SP by itself has also been shown to stimulate inflammatory cytokine production in monocytes, macrophages, and Mast cells, which can further augment the inflammatory response.[53] CGRP, on the other hand, might have modulatory actions on lymphocyte differentiation and cytokine production by macrophages and dendritic cells in response to tissue injury.[30,54,55] A recent study demonstrated SP stimulation of primary human Mast cells and degranulation of cultured Mast cells, while CGRP had no effect on Mast cell degranulation.[56] Since we observed reduced HO in SP and CGRP co-delivered tendons, we speculate that CGRP acted as a modulator of these SP-induced inflammatory responses.

Mast cells have been particularly linked to HO induction in muscle tissue, where in one study by Salisbury et al.,[14] use of a Mast cell stabilizer significantly reduced HO formation. Furthermore, genetic down-regulation of the Mast cells expressing the SP receptor, Neurokinin-1, receptor led to a dramatic reduction in HO.[15] In order to assess whether the pathophysiology in tendon also involves Mast cell activation through the neuropeptides, we investigated the presence of Mast cells in the treated tendons. We observed Mast cell granules within the skin and the connective tissue, which do not have relevance to the HO induction. We also observed positive staining in the ADM, but this was potentially due to a foreign body response. In addition, no marked difference was noted in different treatment types compared to the control animals, supporting this premise.

HO formation has been also associated with inflammatory macrophage accumulation upon tissue injury. Calcified samples of rotator cuff tendon exhibited both dramatic vascularization and neuronal ingrowth along with infiltration of inflammatory macrophages

and Mast cells in the tissue.[57] Additionally, two recent studies showed marked decrease in HO via chemical and genetic depletion of inflammatory macrophages.[17,34] We did not observe macrophage infiltration in the tendon, but only observed a few cells in the ADM and the paratenon. However, it is possible that inflammation cleared out and therefore both the macrophages and the Mast cells were not visible within or around the tendon tissue after 6 weeks or showed no difference with different treatments at this time-point. Further understanding of the neuropeptide-mediated responses through the HO pathophysiology can be achieved by histological analysis at earlier time-points; however, this study investigated the effects of the neuropeptides through a longer time-course since the focus was to identify their roles in HO induction.

We also investigated the effects of these neuropeptides on BMP2 expression. Other groups have shown delivery of exogenous BMP2 induces HO in various animal models of HO. [14,35,58] In this study, BMP2 staining was positive in all treatment groups. SP-treated tendons showed localized expression around the heterotopic bones and chondrocytes, leading to an overall higher expression of BMP2 in these tendons. While only the expression of BMP2 was investigated in this study, but not other BMPs or downstream elements of BMP2 signaling, it is not certain whether co-delivery of SP and CGRP led to a down-regulation in BMP2 signaling. However, the two neuropeptides, when co-delivered, likely to interact through modulatory pathways downstream of the BMP2 pathway to regulate HO formation. It has been reported that SP induces proliferation and matrix adhesion in murine chondrocytes, therefore it can promote terminal differentiation of chondrocytes to osteoblasts during endochondral ossification.[59] CGRP, on the other hand, can delay chondrocyte hypertrophy and matrix mineralization, hence it was suggested to suppress endochondral ossification by up-regulating cAMP levels.[59] A previous in vitro study showed that CGRP interacts with BMP2 signaling in human osteoblast-like cells through up-regulation of cAMP levels to induce osteogenic differentiation.[37] Therefore, in our model we propose that even though CGRP can increase BMP2 expression and chondrocyte differentiation, it can still mitigate SP and therefore result in less HO when delivered together with SP. However, the molecular basis of this interaction during the course of HO development remains to be determined.

CONCLUSION

HO is a significant and costly medical problem, impacting patients' quality of life on a daily basis. Current treatment options are limited since the etiology of HO remains unclear due to its relative complexity.[1,5,6,10] To better understand HO pathophysiology, we developed an animal model that used local delivery of neuropeptides SP and CGRP to a targeted tendon site and reliably induced HO at that site. This approach has significant advantages over existing HO models that use genetic modification, administration of exogenous BMP or induce trauma to the tissue,[12,14,34,35,58] which lack precise control over modulation of specific signaling molecules at HO sites, and potentially confound the data interpretation. Using our novel model, we discovered a potential crosstalk between SP and CGRP, where SP promoted HO alone, and CGRP counteracted SP effects in HO induction in tendon. One limitation to this study was the use of a single neuropeptide dosage and a single time-point for analysis of the effects of SP and CGRP in HO pathophysiology. Therefore, the results

presented here are preliminary, and we believe that investigation of the dose- and time-dependent responses is warranted to incorporate these findings into the development of more effective treatments for HO.

ACKNOWLEDGMENTS

REFERENCES

1. Shehab D, Elgazzar AH, Collier BD. 2002 Heterotopic ossification. J Nucl Med 43:346–353. [PubMed: 11884494]

2. Anthonissen J, Ossendorf C, Ritz U, et al. 2014 Animal models for acquired heterotopic ossification. Acta Orthop Belg 80:2–10. [PubMed: 24873078]

3. Kan L, Kessler JA. 2011 Animal models of typical heterotopic ossification. J Biomed Biotechnol 2011:309287. [PubMed: 20981294]

4. Ramirez DM, Ramirez MR, Reginato AM, et al. 2014 Molecular and cellular mechanisms of heterotopic ossification. Histol Histopathol 29:1281–1285. [PubMed: 24796520]

5. Nauth A, Giles E, Potter BK, et al. 2012 Heterotopic ossification in orthopaedic trauma. J Orthop Trauma 26:684–688. [PubMed: 23010648]

6. Sullivan MP, Torres SJ, Mehta S, et al. 2013 Heterotopic ossification after central nervous system trauma: a current review. Bone Joint Res 2:51–57. [PubMed: 23610702]

7. Convente MR, Wang H, Pignolo RJ, et al. 2015 The immunological contribution to heterotopic ossification disorders. Curr Osteoporos Rep 13:116–124. [PubMed: 25687936]

8. Reichel LM, Salisbury E, Moustoukas MJ, et al. 2014 Molecular mechanisms of heterotopic ossification. J Hand Surg Am 39:563–566. [PubMed: 24246757]

9. Kraft CT, Agarwal S, Ranganathan K, et al. 2016 Trauma-induced heterotopic bone formation and the role of the immune system: a review. J Trauma Acute Care Surg 80:156–165. [PubMed: 26491794]

10. Salisbury E, Sonnet C, Heggeness M, et al. 2010 Heterotopic ossification has some nerve. Crit Rev Eukaryot Gene Expr 20:313–324. [PubMed: 21395504]

11. Wang RN, Green J, Wang Z, et al. 2014 Bone Morphogenetic Protein (BMP) signaling in development and human diseases. Genes Dis 1:87–105. [PubMed: 25401122]

12. Bjurholm A, Kreicbergs A, Dahlberg L, et al. 1990 The occurrence of neuropeptides at different stages of DBM-induced heterotopic bone formation. Bone Miner 10: 95–107. [PubMed: 1698491]

13. Bjur D, Alfredson H, Forsgren S. 2005 The innervation pattern of the human Achilles tendon: studies of the normal and tendinosis tendon with markers for general and sensory innervation. Cell Tissue Res 320:201–206. [PubMed: 15702331]

14. Salisbury E, Rodenberg E, Sonnet C, et al. 2011 Sensory nerve induced inflammation contributes to heterotopic ossification. J Cell Biochem 112:2748–2758. [PubMed: 21678472]

15. Kan L, Lounev VY, Pignolo RJ, et al. 2011 Substance P signaling mediates BMP-dependent heterotopic ossification. J Cell Biochem 112:2759–2772. [PubMed: 21748788]

16. Lui PP, Chan LS, Fu SC, et al. 2010 Expression of sensory neuropeptides in tendon is associated with failed healing and activity-related tendon pain in collagenase-induced tendon injury. Am J Sports Med 38:757–764. [PubMed: 20139325]

17. Genet F, Kulina I, Vaquette C, et al. 2015 Neurological heterotopic ossification following spinal cord injury is triggered by macrophage-mediated inflammation in muscle. J Pathol 236:229–240. [PubMed: 25712044]

18. Gotoh M, Hamada K, Yamakawa H, et al. 1998 Increased substance P in subacromial bursa and shoulder pain in rotator cuff diseases. J Orthop Res 16:618–621. [PubMed: 9820287]

19. Messner K, Wei Y, Andersson B, et al. 1999 Rat model of Achilles tendon disorder. A pilot study. Cells Tissues Organs 165:30–39. [PubMed: 10460971]

20. Ackermann PW, Li J, Lundeberg T, et al. 2003 Neuronal plasticity in relation to nociception and healing of rat achilles tendon. J Orthop Res 21:432–441. [PubMed: 12706015]

21. Schubert TE, Weidler C, Lerch K, et al. 2005 Achilles tendinosis is associated with sprouting of substance P positive nerve fibres. Ann Rheum Dis 64:1083–1086. [PubMed: 15958764]

22. Salo P, Bray R, Seerattan R, et al. 2007 Neuropeptides regulate expression of matrix molecule, growth factor and inflammatory mediator mRNA in explants of normal and healing medial collateral ligament. Regul Pept 142:1–6. [PubMed: 17292490]

23. Scott A, Bahr R. 2009 Neuropeptides in tendinopathy. Front Biosci (Landmark Ed) 14:2203–2211. [PubMed: 19273194]

24. Lui PPY, Chan LS, Fu SC, et al. 2010 Expression of sensory neuropeptides in tendon is associated with failed healing and activity-related tendon pain in collagenase-induced tendon injury. Am J Sport Med 38:757–764.

25. Andersson G, Backman LJ, Scott A, et al. 2011 Substance P accelerates hypercellularity and angiogenesis in tendon tissue and enhances paratendinitis in response to Achilles tendon overuse in a tendinopathy model. Br J Sports Med 45:1017–1022. [PubMed: 21540192]

26. Carlsson O, Schizas N, Li J, et al. 2011 Substance P injections enhance tissue proliferation and regulate sensory nerve ingrowth in rat tendon repair. Scand J Med Sci Sports 21:562–569. [PubMed: 20459473]

27. Zhou B, Zhou Y, Tang K. 2014 The effects of substance P on pluripotent tendon cells: an in vitro and in vivo study. J Musculoskelet Neuronal Interact 14:349–358. [PubMed: 25198231]

28. Ackermann PW, Ahmed M, Kreicbergs A. 2002 Early nerve regeneration after achilles tendon rupture—a prerequisite for healing? A study in the rat. J Orthop Res 20:849–856. [PubMed: 12168677]

29. Lian O, Dahl J, Ackermann PW, et al. 2006 Pronociceptive and antinociceptive neuromediators in patellar tendinopathy. Am J Sports Med 34:1801–1808. [PubMed: 16816149]

30. Lundy FT, Linden GJ. 2004 Neuropeptides and neurogenic mechanisms in oral and periodontal inflammation. Crit Rev Oral Biol Med 15:82–98. [PubMed: 15059944]

31. Ackermann PW, Finn A, Ahmed M. 1999 Sensory neuro-peptidergic pattern in tendon, ligament and joint capsule. A study in the rat. Neuroreport 10:2055–2060. [PubMed: 10424674]

32. Backman LJ, Andersson G, Wennstig G, et al. 2011 Endogenous substance P production in the Achilles tendon increases with loading in an in vivo model of tendinopathy-peptidergic elevation preceding tendinosis-like tissue changes. J Musculoskelet Neuronal Interact 11:133–140. [PubMed: 21625050]

33. Lind H, Brudin L, Lindholm L, et al. 1996 Different levels of sensory neuropeptides (calcitonin gene-related peptide and substance P) during and after exercise in man. Clin Physiol 16:73–82. [PubMed: 8867778]

34. Kan L, Liu Y, McGuire TL, et al. 2009 Dysregulation of local stem/progenitor cells as a common cellular mechanism for heterotopic ossification. Stem Cells 27:150–156. [PubMed: 18832590]

35. Liu X, Kang H, Shahnazari M, et al. 2014 A novel mouse model of trauma induced heterotopic ossification. J Orthop Res 32:183–188. [PubMed: 24136593]

36. Fu S, Mei G, Wang Z, et al. 2014 Neuropeptide substance P improves osteoblastic and angiogenic differentiation capacity of bone marrow stem cells in vitro. Biomed Res Int 2014:596023. [PubMed: 25050364]

37. Tian G, Zhang G, Tan YH. 2013 Calcitonin gene-related peptide stimulates BMP-2 expression and the differentiation of human osteoblast-like cells in vitro. Acta Pharmacol Sin 34:1467–1474. [PubMed: 23708553]

38. Campbell PG, Miller ED, Fisher GW, et al. 2005 Engineered spatial patterns of FGF-2 immobilized on fibrin direct cell organization. Biomaterials 26:6762–6770. [PubMed: 15941581]

39. Campbell PG, Weiss LE. 2007 Tissue engineering with the aid of inkjet printers. Expert Opin Biol Ther 7:1123–1127. [PubMed: 17696812]

40. Cooper GM, Miller ED, Decesare GE, et al. 2010 Inkjet-based biopatterning of bone morphogenetic protein-2 to spatially control calvarial bone formation. Tissue Eng Part A 16:1749–1759. [PubMed: 20028232]

41. Miller ED, Fisher GW, Weiss LE, et al. 2006 Dose-dependent cell growth in response to concentration modulated patterns of FGF-2 printed on fibrin. Biomaterials 27:2213–2221. [PubMed: 16325254]

42. Phillippi JA, Miller E, Weiss L, et al. 2008 Microenvironments engineered by inkjet bioprinting spatially direct adult stem cells toward muscle- and bone-like subpopulations. Stem Cells 26:127–134. [PubMed: 17901398]

43. Weiss L, Amon C, Finger S, et al. 2005 Bayesian computer-aided experimental design of heterogenous scaffolds for tissue engineering. Computer-Aided Design 37:1127–1139.

44. Lui PP. 2013 Histopathological changes in tendinopathy-potential roles of BMPs? Rheumatology (Oxford) 52:2116–2126. [PubMed: 23671126]

45. Mukherjee R, Kanti Barman P, Kumar Thatoi P, et al. 2015 Non-classical monocytes display inflammatory features: validation in sepsis and systemic lupus erythematous. Sci Rep 5:13886. [PubMed: 26358827]

46. Mandl M, Schmitz S, Weber C, et al. 2014 Characterization of the CD14++CD16+ monocyte population in human bone marrow. PLoS ONE 9:e112140. [PubMed: 25369328]

47. Rees JD, Stride M, Scott A. 2014 Tendons-time to revisit inflammation. Br J Sports Med 48:1553–1557. [PubMed: 23476034]

48. O'Brien EJ, Frank CB, Shrive NG, et al. 2012 Heterotopic mineralization (ossification or calcification) in tendinopathy or following surgical tendon trauma. Int J Exp Pathol 93:319–331. [PubMed: 22974213]

49. Zhou Y, Zhou B, Tang K. 2015 The effects of substance p on tendinopathy are dose-dependent: an in vitro and in vivo model study. J Nutr Health Aging 19:555–561. [PubMed: 25923486]

50. Burssens P, Steyaert A, Forsyth R, et al. 2005 Exogenously administered substance P and neutral endopeptidase inhibitors stimulate fibroblast proliferation, angiogenesis and collagen organization during Achilles tendon healing. Foot Ankle Int 26:832–839. [PubMed: 16221456]

51. Steyaert A, Burssens P, Forsyth R, et al. 2010 Qualitative analysis of substance P, NK1-receptor and nerve ingrowth in substance P-treated ruptured rat Achilles tendon. Acta Orthop Belg 76:387–395. [PubMed: 20698462]

52. Bring DK, Paulson K, Renstrom P, et al. 2012 Residual substance P levels after capsaicin treatment correlate with tendon repair. Wound Repair Regen 20:50–60. [PubMed: 22276586]

53. O'Connor TM, O'Connell J, O'Brien DI, et al. 2004 The role of substance P in inflammatory disease. J Cell Physiol 201:167–180. [PubMed: 15334652]

54. Holzmann B 2013 Antiinflammatory activities of CGRP modulating innate immune responses in health and disease. Curr Protein Pept Sci 14:268–274. [PubMed: 23745695]

55. Assas BM, Pennock JI, Miyan JA. 2014 Calcitonin gene-related peptide is a key neurotransmitter in the neuro-immune axis. Front Neurosci 8:23. [PubMed: 24592205]

56. Kulka M, Sheen CH, Tancowny BP, et al. 2008 Neuropeptides activate human Mast cell degranulation and chemokine production. Immunology 123:398–410. [PubMed: 17922833]

57. Hackett L, Millar NL, Lam P, et al. 2016 Are the symptoms of calcific tendinitis due to neoinnervation and/or neovascularization? J Bone Joint Surg Am 98:186–192. [PubMed: 26842408]

58. Kang H, Dang AB, Joshi SK, et al. 2014 Novel mouse model of spinal cord injury-induced heterotopic ossification. J Rehabil Res Dev 51:1109–1118. [PubMed: 25436890]

59. Grassel SG. 2014 The role of peripheral nerve fibers and their neurotransmitters in cartilage and bone physiology and pathophysiology. Arthritis Res Ther 16:485. [PubMed: 25789373]
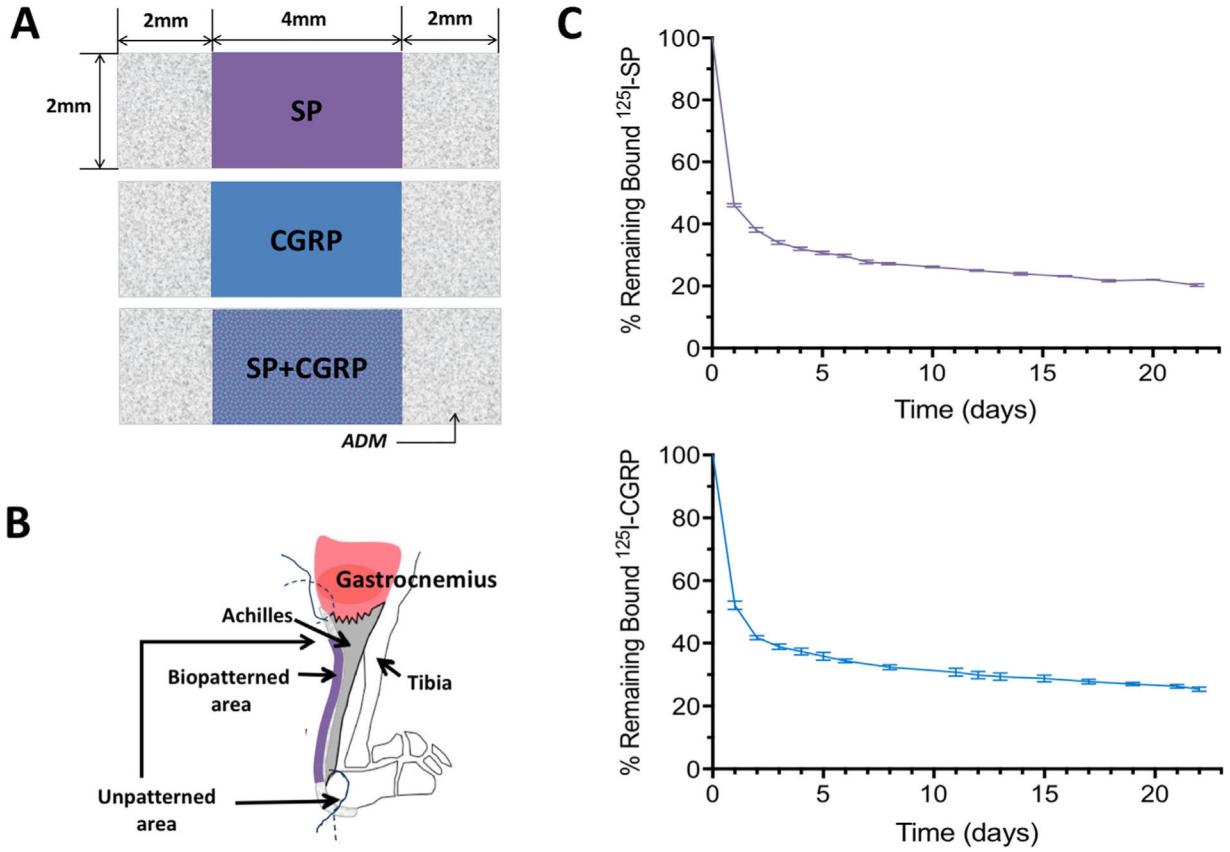
Figure 1.
Implementation of the biopatterned constructs and binding curves for SP and CGRP on ADM (A) Schematics showing ADM constructs with biopatterned treatments. Each construct was 2×8mm with 2×4mm mid-section biopatterned. Control animals received ADM with no treatment. (B) A micro tunnel (0.34mm) was drilled through the calcaneus of the left leg. Biopatterned (with SP, CGRP, or SP + CGRP) or control ADM was implanted with the patterned side facing the Achilles. (C) Binding retention plots of ^{125}I-SP and ^{125}I-CGRP on ADM incubated in simulated in vivo conditions. Each curve represents % of the remaining bound peptide on ADM with ± SEM bars for fourindividual experiments on corresponding days. Approximately 50% of both SP and CGRP were delivered within the first 24 h.
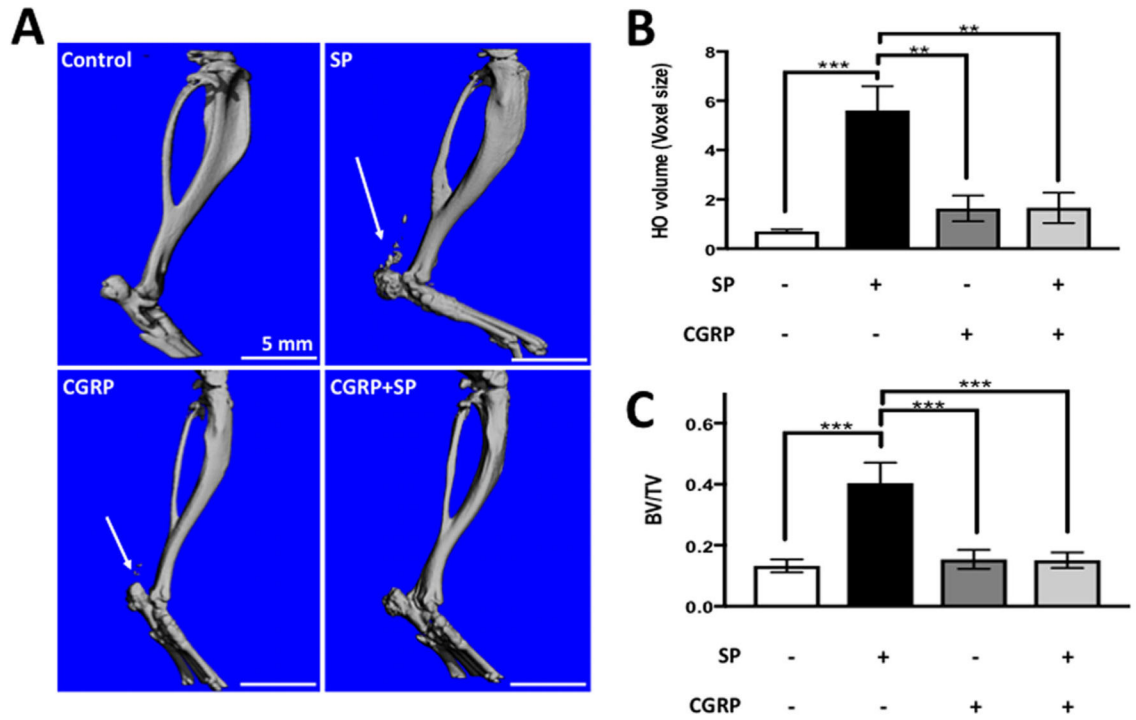
Figure 2.
SP delivery induced HO in Achilles at week 6 post-operation according to the microCT
scans. Co-delivery of SP and CGRP did not exhibit any HO. (A) Representative microCT
images of the treated legs. Scale bars measure 5mm. Arrows point to the HO nodules around
the Achilles. (B) HO around the calcaneus and the Achilles. Bars represent the average HO
volume ± SEM. $n = 6$ per group. (C) HO around the calcaneus and the Achilles. Bars
represent the bone volume (BV)/total volume (TV) ratio ± SEM. Control animals did not
show any HO around the tendon, but the micro hole drilled through the calcaneus was
healed. SP induced significant HO ($p < 0.001$) around the Achilles, while CGRP did not
have a significant effect ($p = 0.9$ compared to the controls, $p < 0.01$ compared to SP-
delivered tendons). Co-delivery of SP and CGRP did not induce HO ($p\mu 0.001$ compared to
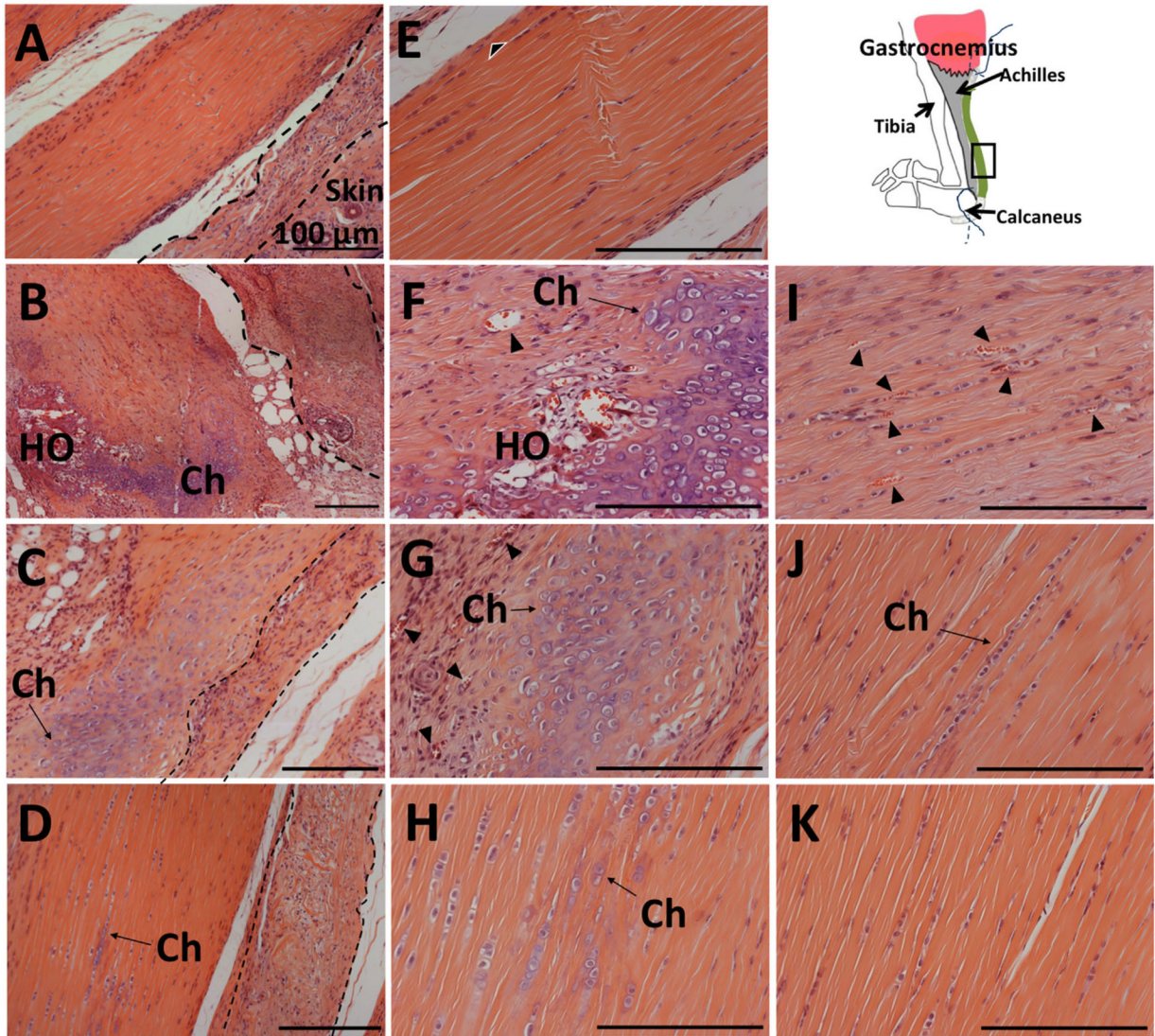SP-delivered tendons).

Figure 3.
Histological analysis of the tendon sections revealed heterotopic bone in SP- and chondrocyte formation in CGRP- or SP + CGRP-delivered tendons. Low magnification images of the Hematoxylin and Eosin (H&E) staining of mid-tendon region in (A) Control, (B) SP, (C) CGRP, (D) SP + CGRP. (E–H), (I–K). Higher magnification of the same H&E stained sections, zoomed into the tendon. Schematic shows the orientation of the images (tendon toward the skin- left to right). ADM is visible next to the tendon (marked with dashed lines), which was infiltrated by mononuclear cells. SP induced degenerative changes in the Achilles, including disorganized collagen, vascularization (marked by black arrowheads), and heterotopic ossification (HO) surrounded by chondrocytes (Ch). CGRP and SP + CGRP led to chondrocyte differentiation (Ch). CGRP also induces vascularization (Black arrowheads). Control tendons did not who show any pathological changes. Cellular proliferation/infiltration was observed around the tendon borders (black and white arrowheads). These regions potentially correspond to paratenon with vascular growth. The proliferation might be a result of surgical trauma. All scale bars measure 100 μm.
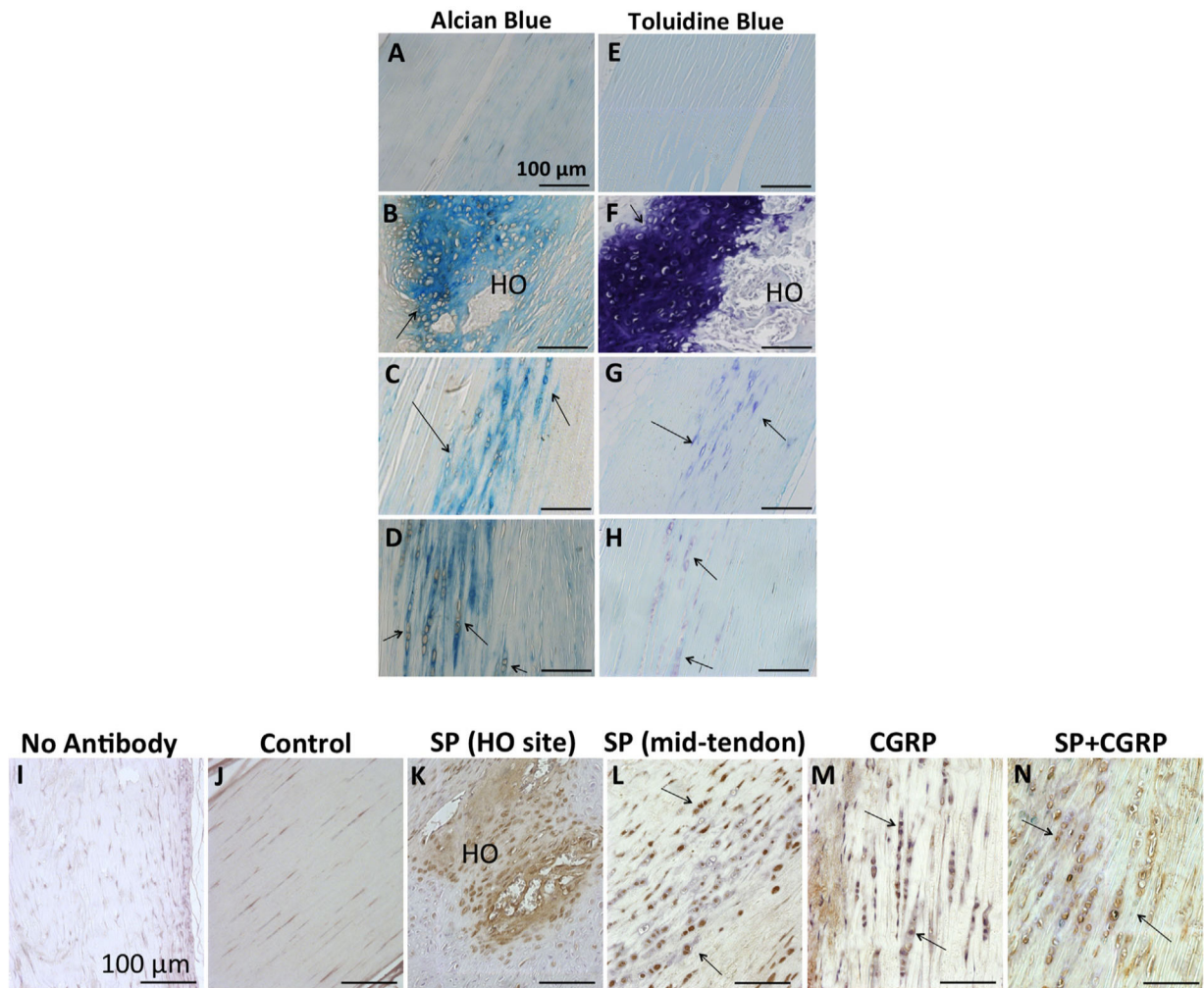
Figure 4.
SP induced HO through endochondral ossification and BMP2 up-regulation. (A–D) Alcian Blue staining, (E–H) Toluidine Blue staining of the mid-tendon sections. Chondrocyte differentiation was confirmed within all legs besides the controls (black arrows). (I–N) Immunostaining for BMP2 (brown). (I) No primary antibody control. (K) BMP2 expression around the HO site in an SP-delivered tendon. (L–N) BMP2 expression in mid-tendons. Higher BMP2 expression was observed around the HO sites (HO) in SP legs, as well as within the chondrocytes (pointed by black arrows) in other treatment groups. All scale bars measure 100μm.
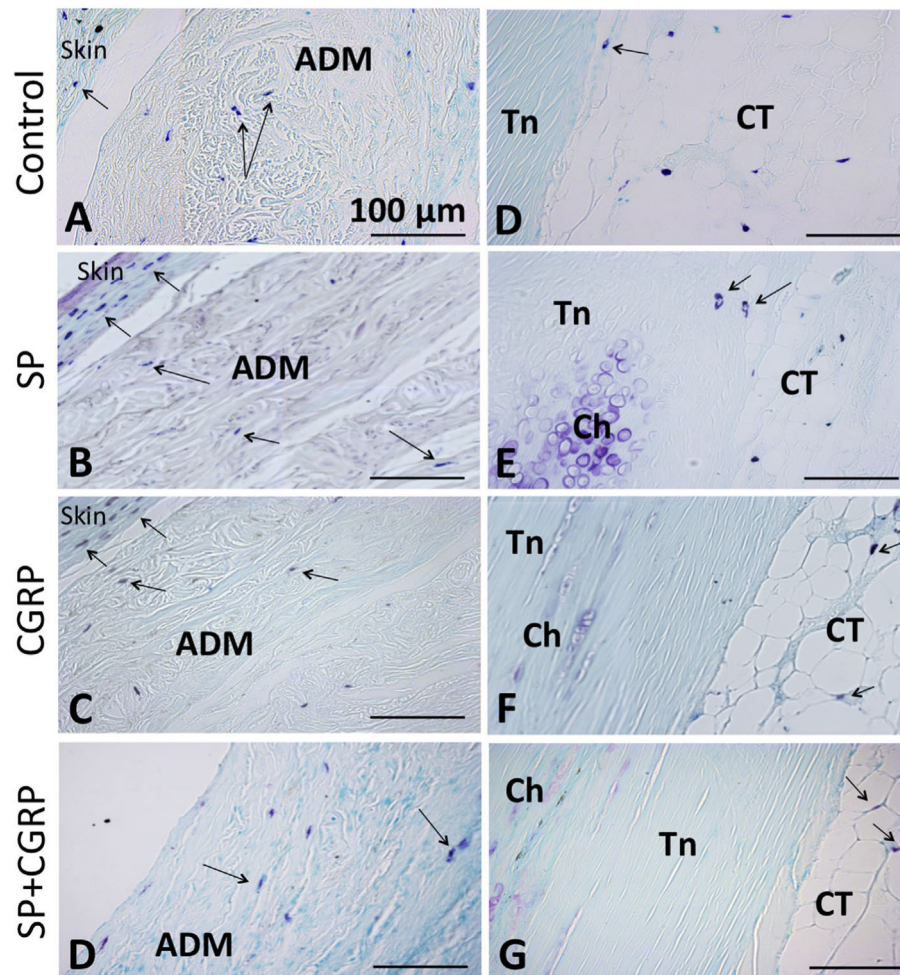
Figure 5.
Mast cell granules (blue-denoted by black arrows) were observed in the skin, the ADM and the connective tissue around, but not within the tendons. Toluidine Blue staining: (A–D) in the ADM, (E–H) by tendon(Tn)-connective tissue (CT) borderline. Chondrocytes (Ch) were also stained by blue as shown in previous figure. All scale bars measure 100μm.
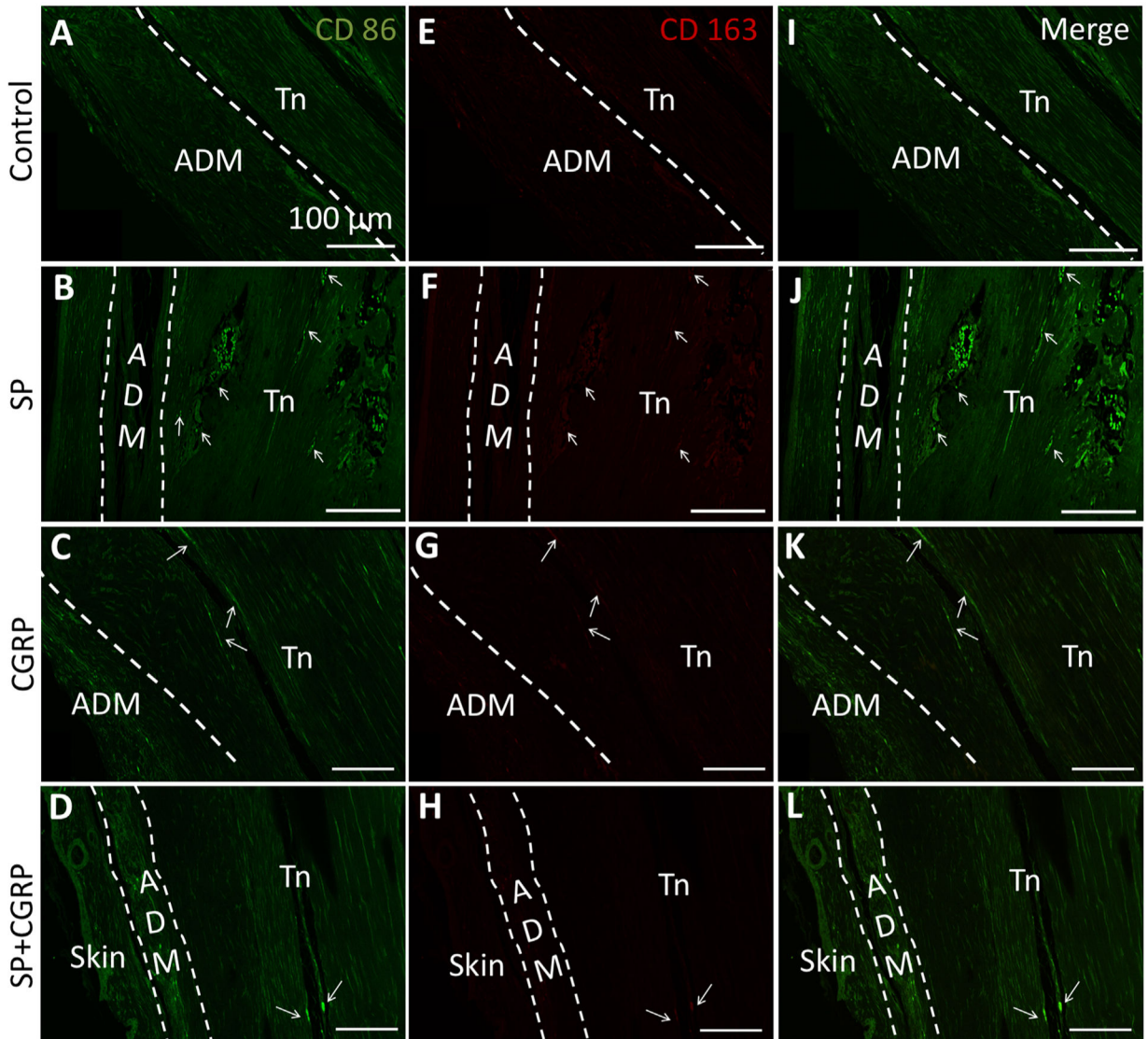
Figure 6.
Macrophage infiltration was not observed in the tendons 6 weeks after treatment delivery. (A–D) Inflammatory (M1:CD86—green), (E–H) Anti-inflammatory (M2:CD163-red), (I–L) Both M1 and M2 macrophage (merge) stainings of the tendons. ADM was marked with white dashed lines. A few M1 positive cells were observed within the ADM in all sections. White arrows denote positive M1 staining in tendons (Tn). M2 staining was negative in these M1-positive areas, also pointed to by white arrows. In controls, CGRP- and SP + CGRP-delivered tendons, these appeared by the tendon borders, and therefore potentially represents the paratenon. In SP-delivered tendons, positive staining was observed within the bone marrow in the HO site and labeled the monocytes residing in these cavities. Additionally, a few more sites with positive staining were observed (white arrows) in these tendons, which might indicate macrophage infiltration through vascularization. However, it is also possible that these sites correspond to small HO sites. Both the ADM and the tendon auto-fluoresced

at Alexa 488 spectrum due to their high collagen composition. All scale bars measure 100μm.

Table 1.

Experimental Groups With Total Deposited Amount of Corresponding Treatment and the Number of Animals Used for Each Group (n)

Treatment Groups	Total Deposited Amount of Peptide (ng/mm^2)	n
Control	–	6
SP	~47	6
CGRP	~47	6
SP + CGRP	~94 (47/each)	6